Korean J. Chem. Eng., 32(2), 268-273 (2015)
DOI: 10.1007/s11814-014-0238-5

pISSN: 0256-1115
eISSN: 1975-7220

Catalytic ozonation of methylene blue in aqueous solution by loading transition metal(Co/Cu/Fe/Mn) on carbon

Fu Huang*, Minghan Luo, Longzhe Cui*, and Guiping Wu*,†**

*Key Laboratory of Catalysis and Materials Science of Hubei Province, College of Chemical and Material Science, South-Central University for Nationalities, Wuhan, Hubei Province 430074, P. R. China
**State Key Laboratory of Urban and Regional Ecology, Research Center for Eco-Environmental Sciences, Chinese Academy of Sciences, Beijing 100085, China
(*Received 16 December 2013 • accepted 19 August 2014*)

Abstract−Activated carbon(AC) was prepared using brewing yeast as a precursor by chemical activation; meanwhile, cobalt, copper, ferrum and manganese supported on activated carbon(Co/AC, Cu/AC, Fe/AC, Mn/AC) were prepared by adsorption-activation method. The characterizations of prepared AC, Co/AC, Cu/AC, Fe/AC, Mn/AC and their performance as ozonation catalysts were tested. The total BET surface areas of prepared AC, Co/AC, Cu/AC, Fe/AC, Mn/AC were found to be 957.7, 789.7, 485.3, 486.1 and 529.8 m^2/g. Absorption capacities of methylene blue (MB) were determined to 407.77, 206.52, 121.25, 123.01, 170.94 mg/g, respectively. The presence of AC was advantageous for TOC reduction of MB compared with UV/O_3 system, and metal Co, Cu, Fe, Mn play an important role in the degradation process. The greatest TOC removal efficiency was obtained in the presence of Co/AC.

Keywords: Catalytic Ozonation, Activated Carbon, Transition Metal, Adsorption, Methylene Blue

INTRODUCTION

Dyes are widely used in the textile industry, which is one of the main sources of industrial waste water, with large amounts, complex components, high content of organic pollutants, strong alkali, poor biodegradability, etc. This kind of wastewater is very difficult to decompose. Since the organic dyestuffs are harmful to people and poisonous to microorganisms without any prior treatment, the removal of dyestuffs from wastewater has received considerable attention [1,2]. A number of ways, such as physical, chemical and biological, have been used for the removal of dyestuffs wastewater [3-6]. The common water treatment methods (adsorption, sedimentation, coagulation, etc.) are now being supplemented by advanced oxidation processes (AOPs). The widely used AOPs include photolysis, Fenton method, photofenton, ozonolysis, sonolysis, and photocatalysis [7,8]. All these treatment methods are versatile and have their own pros and cons. However, in homogeneous/heterogeneous photocatalytic ozonation, one can use the available source of UV radiation from a UV lamp, and in the presence of a suitable catalyst (such as activated carbon catalyst) conduct a chemical reaction to degrade the organic pollutant present in wastewater. Loading the transition metals activated carbon are amongst the most frequently studied ozonation catalysts [9,10]. In a slurry reactor, the mass-transfer-limited reaction can be significantly improved either by increasing gas-liquid mass transfer coefficient or specific surface area [11]. Activated carbon catalyst is inexpensive, environmentally friendly with wonderful adsorption capabilities, and can be easily dispersed in water.

In this work, the AC was prepared using brewing yeast as a precursor by chemical activation with Na_2CO_3 activating agent, and cobalt, copper, ferrum and manganese, supported on activated carbon (Co/AC, Cu/AC, Fe/AC, Mn/AC) was prepared by the adsorption-activation method. The prepared AC and Co/AC, Cu/AC, Fe/AC, Mn/AC were characterized by FTIR spectra, X-ray photoelectron spectroscopy (XPS) and adsorption experiments. The model dye selected for this study was methylene blue (MB). The effect of activated carbon catalysts on the decoloration rate and total organic carbon (TOC) was investigated, and the whole ozonation process was calculated by UV-vis spectroscopy and TOC analyzer. A hypothetical mechanism of MB degradation was also discussed.

EXPERIMENTAL

1. Chemicals and Materials

Brewing yeast used as a precursor was obtained from a brewery in Hubei Province of China. To remove impurities, brewing yeast was washed several times by distilled water, dried at 60 °C for 24 h, ground to a size less than 0.15 mm, then stored in a desiccator. MB (methylene blue, chemical formula $C_{16}H_{18}C_lN_3S$ and λ_{max}= 665 nm) and other chemicals were purchased from Sinopharm Chemical Agent co., Ltd. (Wuhan China). All the chemicals and materials were of analytical grade and used without further purification, except brewing yeast.

The AC was prepared using brewing yeast as a precursor by chemical activation with Na_2CO_3 activating agent. Before its chemical activation, brewing yeast was mixed with Na_2CO_3 at a ratio of 4 : 1 (w/w, brewing yeast: Na_2CO_3), and then the mixture was placed in a sealed ceramic crucible and kept in a muffle furnace at 700 °C

†To whom correspondence should be addressed.
E-mail: wuguiping75@hotmail.com

for 4 h. After the activating treatment, the carbon was cooled and washed with 10% of dilute hydrochloric acid solution and distilled water until neutral pH was observed. The washed samples were dried at 120 °C for 2 h to obtain activated carbon products. This product was designated as AC.

The cobalt, copper , ferrum and manganese supported on activated carbon (Co/AC, Cu/AC, Fe/AC, Mn/AC) were prepared by the adsorption-activation method. Eighty grams of brewing yeast was immersed in 400 mL of cobalt nitrate, manganese chloride, copper nitrate and ferrum nitrate solution with Co^{2+}, Cu^{2+}, Fe^{3+}, Mn^{2+} concentration of 2,000 mg/L for shaking overnight, then filtrated and dried at 60 °C. After that, it was treated by the same way of prepared AC to obtain the required Co/AC, Cu/AC, Fe/AC, Mn/AC.

2. Structural Study of Catalysts

To prove the presence of the transition metals was supported on the surface of the activated carbon, FTIR spectra were recorded by dispersing the glass powders in KBr with a NEXUS-470 FTIR spectrometer (Thermo Nicolet, US) where the spectra were recorded from 400 to 4,000 cm^{-1}. X-ray photoelectron spectroscopy (XPS) measurements were performed using a VG Multilab 2000 electron spectrometer with monochromated Mg Kα radiation (hν=1,253.6 eV). All XPS spectra were corrected using the main C1s peak at 284.6 eV. Curve fitting and background subtraction were accomplished using Elemental Analyzer (PE24002II, USA). The specific surface area and pore structure parameters of activated carbon were determined from the adsorption-desorption isotherm of nitrogen at 77 K using an automated volumetric system (Autosorb-1-C-TCD-MS-Quantachrome Instruments).

3. Adsorption of Methylene Blue

A stock solution of MB was prepared (1,000 mg/*l*). The stock solution was diluted with distilled water to obtain the desired concentration ranging from 100 to 1,000 mg/*l*. Batch adsorption experiments were performed by contacting 0.1 g of the activated carbon catalysts with 100 ml of the MB aqueous solution of different initial concentrations (50, 100, 200, 300, 400, 500, 800, 1,000 mg/*l*). The pH of the solution was adjusted to be 7 using either 0.1 mol/L HCl or NaOH during the adsorption tests. The mixture was shaken at 160 rpm at 25 °C for 4 h. Then samples were taken out and separated by centrifugation at 4,000 rpm for 10 min. The remaining concentration of MB in each sample after adsorption at different time intervals was determined by UV-visible spectrophotometer (UV-2450; Shimadzu, Kyoto, Japan) at a maximum wavelength of 665 nm. MB adsorption mass (q_e) was evaluated according to

$$q_e=(C_i-C_e)V/W \quad (1)$$

where C_i and C_e are the initial and equilibrium concentrations (mg/*l*) of MB solution, respectively; V is the volume (L); and W is the weight (g) of the adsorbent.

4. Catalytic Oxidation Experiments

Similarly, catalytic activity of AC and XX/AC (XX represent Co, Mn, Cu, Fe) was evaluated by comparing the degradation efficiencies of MB solution with three different systems: UV/O3, UV/O_3/AC and UV/O_3/XX/AC. The catalytic ozonation system (Fig. 1) consisted of a tubular glass ozonation reactor (h=450 mm, Φm=70 mm) equipped with gas inlet and outlet and UV lamp (h=350 mm, Φm=15 mm) that was used as a radiation source. Ozone was produced from O_2 by an ozone generator (SK-CFG-20P). Ozonized air (1.5 L/min) was continuously bubbled into the solution and flowed upward in the tubular reactor. The excess ozone in the outlet gas was removed by KI solution. A total of 1.6 g of the catalyst (AC or XX/AC) was added into 1,000 mL of MB aqueous solution (initial concentration 1,400 mg/L). Samples were taken at given intervals to analyze the variation of total organic carbon (TOC) concentrations by a TOC analyzer (Multi N/C 3100, Germany).

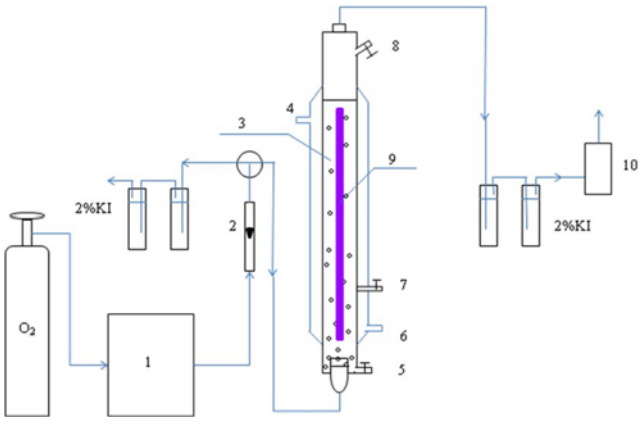

Fig. 1. Diagram of the experimental setup.

1. Ozone generator	6. Inlet of circulation water
2. Flowmeter	7. Sampling
3. Ozonation reactor	8. Inlet of solution
4. Outlet of circulation	9. UV lamp
5. Outlet of solution	10. Ozone destructor

RESULTS AND DISCUSSION

1. Characterization of Prepared Catalysts

Fig. 2 displays the FTIR spectra of prepared AC, Co/AC, Cu/AC, Fe/AC, Mn/AC. According to the literature [12,13], evidently, the spectrum of the hydroxyl stretching region showed a broad band

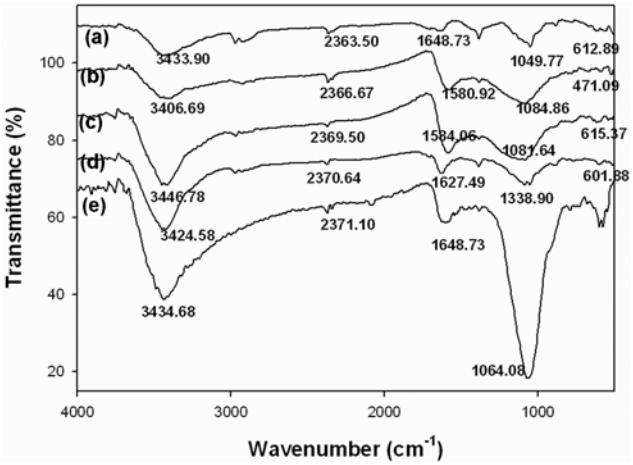

Fig. 2. The FTIR spectra of Co/AC (a), Mn/AC (b), Cu/AC (c), Fe/AC (d), AC (e).

in the region of 3,200-3,600 cm^{-1}; 1,648-1,580 cm^{-1} absorption peak confirmed the presence of amine; 2,363-2,371 cm^{-1} is caused by vibration of carbonyl; the vibration of -C-O is reflected at 1,038-1,084 cm^{-1} at room temperature. Moreover the IR absorbance of Co/AC(a) due to the spinal Co-O bond was observed at 612 cm^{-1} which corresponds to Co_3O_4 crystallite formed within support [14]. With the addition of MnO_2 content, the band which wave number was 471 cm^{-1} was also noticed in sample of Mn/AC(b) and the band was observed wave number (615 cm^{-1}) side in the sample of Cu/AC(c) with an increase in the percentage of Cu-O [15,16]. Finally, with the addition of Fe-O content, the band which wave number was 537 cm^{-1} was also noticed in the sample of Fe/AC(d) [17]. In total, the transition metals were successfully loaded onto the activated carbon by comparing FTIR spectra of the five catalysts.

X-ray photoelectron spectroscopy (XPS) over a large energy range at low resolution was used to study the elements present in Co/AC, Cu/AC, Fe/AC, Mn/AC and AC, and the binding energy was calibrated using the C1s signal (284.6 eV) and O1s for oxygen (531.6 eV) from the coating surface of each activated carbon catalysts. It was unambiguously observed that O, C and the transition metals elements exist in the samples, as shown in Fig. 3. The existing form of $Co2p_{3/2}$ and $Co2p_{1/2}$ is Co_3O_4 since their binding energies are close to 781.2 and 796.5 eV (Fig. 3(a)), with a binding energy difference of 15.3 eV, which is similar to the reference [18]. The Mn_{2p} XPS spectra show two major peaks with binding energies at 643.7 and 654.3 eV, corresponding to $Mn_{2p3/2}$ and $Mn2p_{1/2}$, respectively, with a spin-energy separation of 25 eV (Fig. 3(b)), which is the characteristic of a Mn_3O_4 phase and in good agreement with the reported data [19]. The existing form of Cu_{2p} is CuO since its binding energy is close to 933.7 eV (Fig. 3(c)), which is the characteristic of a CuO phase and in good agreement with the reported data [20]. It can be seen clearly that two separated 2p electron orbital energy states of $Fe2p_{3/2}$ and $Fe2p_{1/2}$ peaks are centered at 712.6 and 724.2 eV (Fig. 3(d)), which is similar to the reference. This result was consistent with the FTIR analysis as mentioned above.

It was found that the BET surface areas of prepared AC, Co/AC, Cu/AC Fe/AC and Mn/AC were 957.7, 789.7, 485.3, 486.1 and 529.8 m^2/g with total pore volumes of 0.81, 0.67, 0.45, 0.75 and 0.47 ml/g, average pore diameters of 4.9, 3.4, 3.7, 3.8 and 3.5 nm, respectively. Compared to AC, the metal-AC showed significantly lower BET surface area and pore volume as well as slightly smaller average pore size. One possible reason is that part of the metal atoms entered into the pore of the support and blocked pores, or the metal atoms stayed at the surface of AC and reduced the surface area.

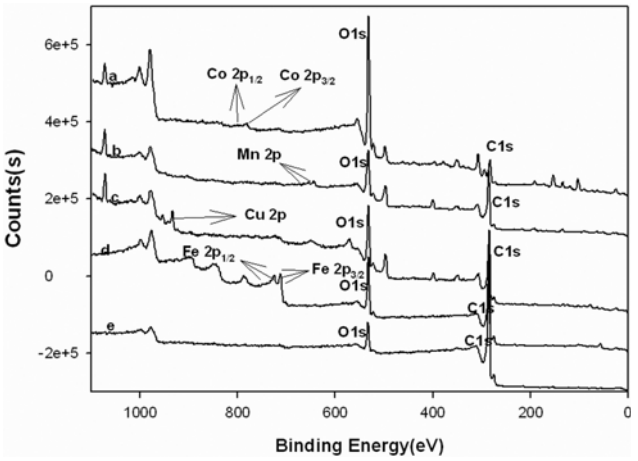

Fig. 3. XPS Spectrums of Co/AC (a), Mn/AC (b), Cu/AC (c), Fe/AC (d), AC (e).

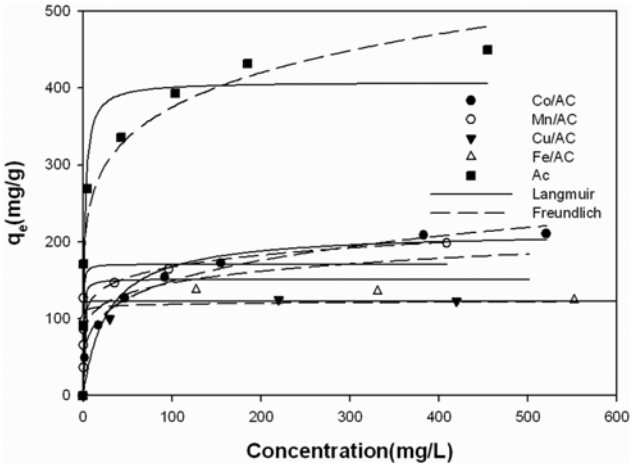

Fig. 4. Adsorption isotherms of MB on AC, Co/AC, Mn/AC, Cu/AC and Fe/AC. Solid and dotted lines represent Langmuir equation and Freundlich equation, respectively. Circles represent Co/AC (black) and Mn/AC (white), respectively. Triangles represent Cu/AC (black) and Fe/AC (white). Squares represent AC (black). Solution volume and adsorbent dosage are 100 mL and 0.1 g. Solid line is predicted from Langmuir parameters given in Table1.

2. Adsorption Isotherms

Fig. 4 shows the adsorption isotherms of MB by AC, Co/AC, Cu/AC, Fe/AC and Mn/AC, respectively. As can be seen, the amount of MB adsorbed onto AC increased with equilibrium concentration (C_e) at first and then reached to the maximum value. In this study, the Langmuir (Eq. (2)) and Freundlich (Eq. (3)) [21] were used to fit the experimental data. The Langmuir and Freundlich parameters, along with correlation coefficients (R^2), were estimated using nonlinear regression method (Fig. 4) and summarized in Table 1. It can be seen that the maximum (q_m) uptake of MB by AC, Co/AC, Cu/AC, Fe/ACand Mn/AC was estimated to be 407.77, 206.52, 121.25, 123.01 and 170.94 mg/g, respectively. Compared with AC, there is an obvious decrease in adsorption capability of metal/AC. This was also proved by the results of BET surface area. The reason was likely to be the presence of metal effect on the activating process of AC.

Table 2 lists the comparison of maximum adsorption capacity of some dyes on various adsorbents. Compared with the data in the literature, the activated carbon studied in this work has very large adsorption capacity.

$$\text{Langmuir equation: } q_e = \frac{q_m K_a C_e}{1 + K_a C_e} \quad (2)$$

where C_e represents the equilibrium concentration of MB (mg/L), q_e and q_m are the equilibrium and maximum adsorption capacity (mg/g), K_a is the Langmuir constants.

Table 1. Parameters for adsorption isotherms of MB on AC, Co/AC, Mn/AC, Cu/AC and Fe/AC

Material	Langmuir model			Freundlich model		
	q_m/(mg/g)	K_a	R^2	K_F	n	R^2
AC	407.77 (28.235)	0.571 (0.251)	0.909	177.46 (22.572)	6.146 (0.983)	0.946
Co/AC	206.52 (5.7698)	0.076 (0.010)	0.961	218.24 (3.3952)	0.001 (0.0001)	0.991
Mn/AC	170.94 (11.565)	3.906 (1.158)	0.923	94.25 (10.2043)	8.018 (1.531)	0.906
Cu/AC	121.25 (4.078)	0.112 (0.055)	0.984	87.76 (16.7796)	21.11 (14.340)	0.975
Fe/AC	123.01 (5.472)	21.77 (15.17)	0.944	109.47 (11.1140)	57.583 (58.35)	0.928

Table 2. Comparison of the maximum monolayer adsorption of some dyes on various adsorbent

Dyes	Adsorbent	Maximum monolayer adsorption capacity (mg/g)	References
Methylene blue	Brewing yeast AC	407.77	This work
Methylene blue	Posidonia oceanic AC	285.70	[22]
Methylene blue	Coconut husk AC	434.78	[23]
Methylene blue	Oil palm fibre AC	277.78	[24]
Methylene blue	Durian shell AC	289.26	[25]
Methylene blue	Date stones AC	316.11	[26]
Methylene blue	Date palm pits AC	455.00	[27]
Methylene blue	Orange peel AC	382.75	[28]
Methylene blue	Jute fiber AC	225.64	[29]
Methylene blue	Bamboo-based AC	454.20	[30]
Basic red 46	Sludge-based AC	188.00	[31]
Acid brown 283	Sludge-based AC	20.50	[31]
Direct red 89	Sludge-based AC	49.20	[31]
Direct black 168	Sludge-based AC	28.90	[31]
Basic red 46	Chemviron GW AC	106.00	[31]
Acid brown 283	Chemviron GW AC	22.00	[31]
Direct red 89	Chemviron GW AC	8.40	[31]
Direct black 168	Chemviron GW AC	18.70	[31]
Congo red	Coir pith-based AC	6.72	[32]

Freundlich equation: $q_e = K_F C_e^{1/n}$ (3)

where K_F and 1/n are empirical constants, C_e represents the equilibrium concentration of MB (mg/L), q_e is the equilibrium adsorption capacity (mg/g).

3. Catalytic Ozonation of MB

The prepared AC, Co/AC, Cu/AC, Fe/AC and Mn/AC were used as catalysts in UV assisted catalytic ozonation systems. To evaluate the catalytic activities of these five catalysts, the variations of MB removal efficiencies and TOC removal efficiencies were compared under six systems: UV/O_3, AC/UV/O_3, Co/AC/UV/O_3, Cu/AC/UV/O_3, Fe/AC/UV/O_3 and Mn/AC/UV/O_3. To take the effect of adsorption into consideration, the mixture of catalyst and MB aqueous solution was first stirred for 24 h without ozone and UV. Then 3.0 ml of mixture was drawn out as the sample of 0 min.

In this work, the MB removal efficiency was checked by measuring the MB concentration of the solution by UV-visible spectrophotometer. It can be seen from Fig. 5(a) that there is no significant different for MB removal efficiencies of UV/O_3, AC/UV/O_3, Co/AC/UV/O_3, Cu/AC/UV/O_3, Fe/AC/UV/O_3 and Mn/AC/UV/O_3 systems. The removal efficiencies of MB reached about 100% within 20 min, and the color of the solution completely faded too.

However, the color fading of the solution did not mean the complete degradation of MB. The mineralization was checked by measuring the TOC of the solution. The removal efficiencies of TOC along with reaction time under six systems are shown in Fig. 5(b). It can be seen from Fig. 5(b) that the presence of catalysts accelerated the removal of TOC. After reaction of 120 min, TOC removal rate reached 35.93%, 41.86%, 80.39% 52.80%, 43.94%, 62.25% in the system of UV/O_3, AC/UV/O_3, Co/AC/UV/O_3, Cu/AC/UV/O_3, Fe/AC/UV/O_3 and Mn/AC/UV/O_3, respectively. The results in Fig. 5(b) show that the greatest TOC removal rate was obtained in presence of Co/AC, then Mn/AC, Cu/AC, Fe/AC and AC.

The results indicate that the presence of AC improved the TOC removal efficiency. The contribution of AC can be partly ascribed to the following two possible reasons: (1) AC can provide a high specific surface area, so both organic compounds and ozone can be adsorbed and reacted on it; (2) it can accelerate the transformation of ozone with large amount of .OH radicals generated under the irradiation of ultraviolet light [33].

The higher TOC removal efficiency was obtained in the case of metal/AC/UV/O_3. This demonstrates that the catalytic activity of

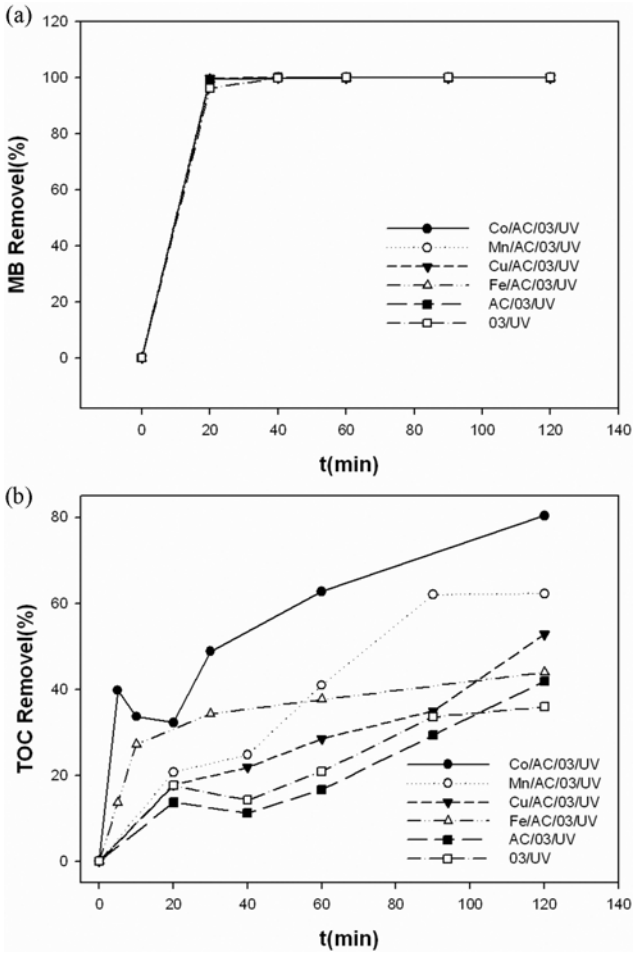

Fig. 5. Effect of catalysts on removal of MB (a) and TOC (b). Ozone dose: 1,080 mg/h, catalyst dose: 1.6 g, initial concentration of MB solution: 1,400 mg/L, volume of MB solution: 1 L, temperature: 25 °C, flow rate of oxygen: 1.5 L/min.

metal/AC is higher than that of AC. As mentioned in the previous sections, the BET surface area and adsorption capacity of metal/AC exhibited lower compared with AC. Therefore, the presence of metal in AC plays an important role in the degradation process. The surface of metal/AC potentially has more active sites, which enhances the transformation of ozone with large amount of .OH radical generation. It is well known that .OH radical is a very powerful and nonselective oxidizing agent that can deal with organic compounds until mineralized.

Comparing the TOC removal efficiencies of the system of Co/AC/UV/O_3, Cu/AC/UV/O_3, Fe/AC/UV/O_3 and Mn/AC/UV/O_3, the effect of Co/AC catalytic activity was optimal in this process.

4. Mechanism Analysis

In the aqueous solution, MB was catalyzing ozonation by catalyst, and it was first decomposed into aromatic hydrocarbons and heterocyclic compounds, eventually degraded into small molecule esters and acids under the action of ozone and UV, catalyst generated hydroxyl radicals. Wherein the hydroxyl radicals play an important role in the degradation of organic matter, during the reaction process, it produced some inert materials to inhibit ozone and hydroxyl radicals, and the inert materials were not easy to be further degraded. Furthermore these substances can hinder further hydroxyl radical chain reactions on catalytic ozonation process inhibiting degradation of organic matter. The degradation process contains four possible degradation mechanisms [34,35].

(1) Direct oxidation by the ozone molecule; ozone reacts selectively directly with the organic matter in water.

$$O_3 + MB \rightarrow P$$

(2) Ozone is decomposed into hydroxyl radicals under UV irradiation, oxidized non-selectively organic matter.

$$O_3 + H_2O \xrightarrow{h\nu} H_2O_2 + O_2$$
$$H_2O_2 \xrightarrow{h\nu} 2HO\bullet$$

(3) Radical oxidation by highly oxidative free radicals such as hydroxyl free radicals, which are formed by decomposition of ozone under the catalyst in the aqueous solution.

$$OH^- + S \Leftrightarrow OH - S$$
$$O_3 + OH - S \Leftrightarrow \bullet O_3 - S + OH\bullet$$
$$\bullet O_3 - S \Leftrightarrow \bullet O - S + O_2$$
$$O_3 + \bullet O - S \Leftrightarrow O_2\bullet^- + S + O_2$$

(4) Interface effect mechanism: MB, reaction intermediates, and hydroxyl radicals and ozone adsorbed on the catalyst surface, interacting, oxidative degradation of organic materials is to produce degradation products and fall off.

$$O_3 + S \Leftrightarrow O_3 - S$$
$$MB + S \Leftrightarrow MB - S$$
$$MB - S + O_3 - S \Leftrightarrow P - S$$

CONCLUSIONS

This study focused on the preparation of transition metal activated carbon catalysts to be used in the removal of dyestuffs water by ozonation. In summary, AC was prepared using brewing yeast as a precursor by chemical activation with Na_2CO_3 activating agent, and transition metal supported on activated carbon was prepared by the adsorption-activation method. The FTIR and XPS results showed that the transition metals were successfully loaded onto the activated carbon.

The BET surface areas of prepared AC, Co/AC, Cu/AC, Fe/AC, Mn/AC were found to be 957.7, 789.7, 485.3, 486.1 and 529.8 m^2/g. The maximum uptake (q_m) of MB by AC, Co/AC, Cu/AC, Fe/AC, Mn/AC was estimated to be 407.77, 206.52, 121.25, 123.01, 170.94 mg/g, respectively. The catalytic photolytic ozonation process was much more efficient than the individual photolytic ozonation process for decolorizing this dye. Examination of the effects of various transition metal AC showed that the TOC reduction ultimately reached 80.39%, 62.25%, 52.80% and 43.94% for Co/AC, Cu/AC, Fe/AC and Mn/AC, respectively. The effect of Co/AC catalytic is optimal.

ACKNOWLEDGEMENT

This work was supported by a grant of the Research and Devel-

opment Program, Hubei province, Science and Technology Department (2008BCD202) and Scientific Research Foundation for the returned overseas.

REFERENCES

1. K. Bhattacharyya and A. Sharma, *Dyes Pigm.*, **65**, 51 (2005).
2. A. M. M. Vargas, A. L. Cazetta, M. H. Kunita, T. L. Silva and V. C. Almeida, *Chem. Eng. J.*, **168**, 722 (2011).
3. M. Goncalves, M. C. Guerreiro, L. C. de Oliveira and C. S. de Castro, *J. Environ. Manage.*, **127**, 206 (2013).
4. V. K. Gupta, D. Pathania, S. Agarwal and P. Singh, *J. Hazard. Mater.*, **243**, 179 (2012).
5. H. A. Le, L. T. Linh, S. Chin and J. Jurng, *Powder Technol.*, **225**, 167 (2012).
6. G. Wu, T.-s. Jeong, C.-H. Won and L. Cui, *Korean J. Chem. Eng.*, **27**, 1476 (2010).
7. M. A. Rauf, M. A. Meetani, A. Khaleel and A. Ahmed, *Chem. Eng. J.*, **157**, 373 (2010).
8. B. H. Hameed and T. W. Lee, *J. Hazard. Mater.*, **164**, 468 (2009).
9. P. M. Alvárez, F. J. Beltrán, F. J. Masa and J. P. Pocostales, *Appl. Catal. B: Environ.*, **92**, 393 (2009).
10. C. A. Orge, J. J. M. Órfão, M. F. R. Pereira, A. M. Duarte de Farias and M. A. Fraga, *Chem. Eng. J.*, **200**, 499 (2012).
11. S. Piché, B. P. Grandjean, I. Iliuta and F. Larachi, *Environ. Sci. Technol.*, **35**, 4817 (2001).
12. M. A. Corres, M. Zubitur, M. Cortazar and A. Múgica, *J. Anal. Appl. Pyrolysis*, **92**, 407 (2011).
13. A. Danon, P. C. Stair and E. Weitz, *J. Phys. Chem. C*, **115**, 11540 (2011).
14. P. Shukla, H. Sun, S. Wang, H. M. Ang and M. O. Tadé, *Sep. Purif. Technol.*, **77**, 230 (2011).
15. S. P. Hashim, H. A. Sidek, M. K. Halimah, K. A. Matori, W. M. Yusof and M. H. Zaid, *Int. J. Mole. Sci.*, **14**, 1022 (2013).
16. D. P. Dubal, D. S. Dhawale, R. R. Salunkhe, V. S. Jamdade and C. D. Lokhande, *J. Alloys Compd.*, **492**, 26 (2010).
17. S. P. Singh, R. P. S. Chakradhar, J. L. Rao and B. Karmakar, *J. Alloys Compd.*, **493**, 256 (2010).
18. J. Yan, T. Wei, W. Qiao, B. Shao, Q. Zhao, L. Zhang and Z. Fan, *Electrochim. Acta*, **55**, 6973 (2010).
19. A. Moses Ezhil Raj, S. G. Victoria, V. B. Jothy, C. Ravidhas, J. Wollschläger, M. Suendorf, M. Neumann, M. Jayachandran and C. Sanjeeviraja, *Appl. Surf. Sci.*, **256**, 2920 (2010).
20. L. Zhang, S. L. Candelaria, J. Tian, Y. Li, Y.-x. Huang and G. Cao, *J. Power Sources*, **236**, 215 (2013).
21. K. Hall, L. Eagleton, A. Acrivos and T. Vermeulen, *Ind. Eng. Chem. Fundamentals*, **5**, 212 (1966).
22. M. U. Dural, L. Cavas, S. K. Papageorgiou and F. K. Katsaros, *Chem. Eng. J.*, **168**, 77 (2011).
23. I. A. Tan, A. L. Ahmad and B. H. Hameed, *J. Hazard. Mater.*, **337**, 154 (2008).
24. I. A. Tan, B. H. Hameed and A. L. Ahmad, *Chem. Eng. J.*, **127**, 111 (2007).
25. T. C. Chandra, M. M. Mirna, Y. Sudaryanto and S. Ismadji, *Chem. Eng. J.*, **127**, 121 (2007).
26. K. Foo and B. Hameed, *Chem. Eng. J.*, **170**, 338 (2011).
27. K. S. K. Reddy, A. Al Shoaibi and C. Srinivasakannan, *New Carbon Mater.*, **27**, 344 (2012).
28. K. Y. Foo and B. H. Hameed, *Bioresour. Technol.*, **104**, 679 (2012).
29. W. T. Tsai, C. Y. Chang, M. C. Lin, S. F. Chien, H. F. Sun and M. F. Hsieh, *Chemosphere*, **45**, 51 (2001).
30. B. H. Hameed, A. T. Din and A. L. Ahmad, *J. Hazard. Mater.*, **141**, 819 (2007).
31. M. J. Martin, A. Artola, M. D. Balaguer and M. Rigola, *Chem. Eng. J.*, **94**, 231 (2003).
32. C. Namasivayam and D. Kavitha, *Dyes Pigm.*, **54**, 47 (2002).
33. C. A. Guzman-Perez, J. Soltan and J. Robertson, *Sep. Purif. Technol.*, **79**, 8 (2011).
34. Y. H. Chen, C. Y. Chang, C. C. Chen, C. Y. Chiu, Y. H. Yu, P. C. Chiang, C. F. Chang and Y. Ku, *Ind. Eng. Chem. Res.*, **43**, 1932 (2004).
35. J. Staehelin and J. Hoigne, *Environ. Sci. Technol.*, **16**, 676 (1982).